

P-HiL Evaluation of Virtual Inertia Support to the Nordic Power System by an HVDC Terminal

*Salvatore D'Arco

*Thuc Dinh Duong

*†Jon Are Suul

SINTEF Energy Research
Trondheim, Norway
salvatore.darco@sintef.no
thuc.duong@sintef.no

Department of Engineering Cybernetics
Norwegian University of Science and Technology
Trondheim, Norway
Jon.A.Suul@sintef.no

Abstract—This paper provides an assessment of the effect from virtual inertia provided by an HVDC converter terminal on the Nordic power system. The analysis is based on results from Power-Hardware-in-the-Loop (P-HiL) tests with a laboratory-scale Modular Multilevel Converter (MMC) representing an HVDC terminal interfaced with a real-time phasor simulation of the Nordic grid. The applied control method for providing virtual inertia is utilizing the derivative of the locally measured grid frequency to adapt the power reference for the studied converter terminal. The power injection provided by the converter and the resulting impact on the frequency dynamics of the power system are investigated as a function of the emulated inertia constant and the frequency droop gain. The results demonstrate how the HVDC converter can effectively support the dynamic response of the power system when exposed to large load transients by improving the frequency nadir and reducing the Rate-of-Change-of-Frequency (ROCOF).

Keywords—HVDC Transmission, Power-Hardware-in-the-Loop, Real-time Simulation, Virtual Inertia

I. INTRODUCTION

The ongoing developments towards large-scale utilization of converter interfaced generations are leading to concerns regarding declining inertia in traditional power systems [1]-[3]. Currently, such concerns are especially relevant for islanded power systems like in UK and Ireland [4], [5]. However, also operation of larger interconnected power systems can be expected to experience local or system-wide challenges related to declining inertia during the coming decades [6]. In the Nordic power system, potential challenges related to low inertia operation are mainly expected during low-load conditions with high import from HVDC interconnections [7]. If such conditions will occur when there is high production from converter-interfaced generation sources like wind farms, the equivalent system inertia can fall below the limits specified for safe operation of the system. However, the high relative rating of HVDC converters also imply that they can be utilized to mitigate the effects of reduced physical inertia by providing virtual or synthetic inertia.

During the last decade a wide range of studies have proposed various implementations of control strategies for power electronic converters to provide virtual inertia to

This work was supported by the project "HVDC Inertia Provision" (HVDC Pro), financed by the ENERGIX program of the Research Council of Norway (RCN) with project number 268053/E2, and the industry partners; Statnett, Statoil, RTE and ELIA.

power systems by emulating the dynamic characteristics of synchronous machines [8]-[10]. The available literature also includes multiple examples of control concepts proposed for HVDC converter terminals [11]-[15]. However, most publications proposing control strategies for providing virtual inertia have only included verifications of functionality in ideal or very simplified power system configurations. Thus, there is a need for comprehensive testing, analysis and verification under realistic power system conditions before potential widespread application of such control strategies to HVDC systems.

Power-Hardware-in-the-Loop (P-HiL) testing is emerging as a practical approach for conducting physical experiments with converter hardware in combination with real time simulation of power systems, to recreate realistic operating conditions [16]. Indeed, P-HiL testing can allow for obtaining two combined features that cannot be easily provided by offline simulation or experimental tests based only on hardware: i) A simulated power system model can be exposed to the actual dynamics and the practical operational characteristics of a power electronic converter, including effects that cannot be easily or conveniently represented in a large-scale power system simulation. ii) The power converters under test can be exposed to realistic power system operating conditions generated by the real-time simulation, and the interactions between the control system and the dynamics of a large-scale system can be tested in a safe and controlled laboratory environment.

In this paper, P-HiL testing is utilized to assess the impact from virtual inertia support by an HVDC converter terminal on a model of the Nordic power system. The Nordic power system is represented by a 44-bus phasor model, which is simulated in real-time on an OPAL-RT platform. The simulated voltage at a bus where the virtual inertia support should be provided is amplified by a grid emulator interfaced with a scaled MMC prototype representing the HVDC terminal. Similarly, the response of the physical converter is fed back to the real-time simulation, to evaluate the impact from inertia emulation by the converter on the power system. The presented results demonstrate how the equivalent inertia emulated by the HVDC terminal, and the frequency droop included in the control, influences the frequency Nadir and the Rate-of-Change-of-Frequency (ROCOF) in the simulated grid when exposed to a severe load transient. Furthermore, the applied P-HiL configuration can be utilized for conducting a wide range of studies into the potential impact on the Nordic power system from practical control strategies for providing ancillary services from HVDC converter terminals.

stationary reference, with an implementation adapted from the control strategy described in [23].

The outer loop controllers providing the d - and q -axis current references for the ac-side control are conventional active and reactive power control loops based on PI-regulators. However, the active power control loop is enhanced by an incremental power reference Δp_{IE}^* for providing inertia emulation and primary frequency control. This reference is generated by the block labelled as "inertia emulation" in Fig. 2, based on the grid frequency ω_{PLL} detected by the PLL. Since the IE implementation relies on the assumption of an equivalent swing equation, the power to be provided as an inertial response is proportional to the derivative of the measured grid frequency:

$$\Delta p_{IE}^* = -T_a \frac{d\omega_g}{dt} \quad (1)$$

where $T_a = 2H$ is the equivalent inertia to be emulated.

The frequency derivative-based inertia emulation is implemented with a limitation on the bandwidth of the derivative, to avoid amplification of noise. This is obtained by low pass filtering the estimated frequency from the PLL. A grid frequency droop term is also added to the incremental power reference provided by the inertia emulation strategy. Thus, the power reference Δp_{IE}^* can be expressed as:

$$\Delta p_{IE}^* = -T_a \frac{s\omega_{LPf}}{s + \omega_{LPf}} \omega_{PLL} + k_\omega (\omega^* - \omega_{PLL}) \quad (2)$$

Further details on the implementation of the df/dt -based IE strategy for the ac-side control of the converter can be found in [22] and [24].

IV. CONFIGURATION OF LABORATORY SETUP

The experimental tests have been conducted with a laboratory setup as indicated by the schematic in Fig. 3. The setup includes an MMC converter prototype designed as a scaled model of an HVDC converter, according to the information presented in Table I [15]. The MMC is fed from the dc side by a controllable voltage source. On the ac-side, it is connected to the terminals of a high bandwidth switch-mode amplifier which is operated as grid emulator and provides the interface between the real-time simulation and the MMC. This grid emulator and the MMC are both connected to a real-time simulator from OPAL-RT by a low latency optical fiber communication. A picture of the laboratory setup is shown in Fig. 4.

As mentioned in section II, a real-time simulation of the Nordic 44 bus model is utilized for the P-HiL testing. The real-time model is implemented as a phasor simulation in ePHASORSIM on the OPAL-RT platform. The phasor simulation generates in real time the voltage phasor for the node 5500 in Fig. 1 where the HVDC terminal represented by the laboratory scale MMC is assumed to be connected to the grid. This phasor is transformed to a three-phase voltage in the stationary frame and these waveforms are applied as references for the control of the grid emulator [21]. Since the converter is modelled as an active power injection in the simulated grid, the power measured from the converter is fed back in the simulation to obtain the intended PHiL behavior.

The OPAL-RT platform is also utilized to implement the main control loops of the MMC, according to the control structure from Fig. 2. The control system is implemented with a sampling time of 100 μ s. However, the low-level control of the MMC topology, including the modulation and

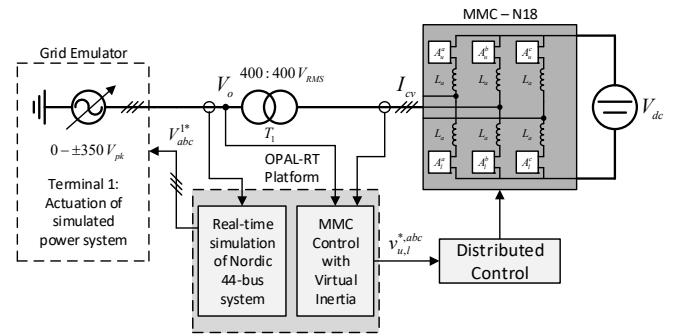


Fig. 3. System configuration for PHiL testing of MMC prototype providing virtual inertia to the Nordic 44-bus system simulated in real-time

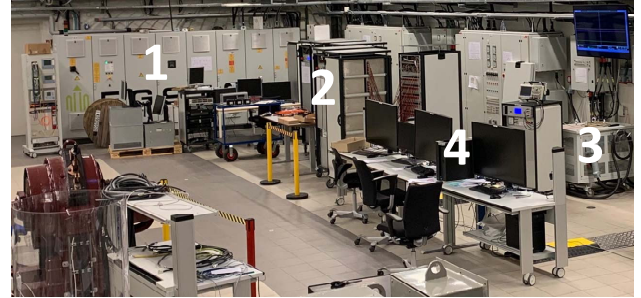


Fig. 4. Picture of laboratory setup with 1) Grid emulator, 2) MMC prototype, 3) transformer, and 4) Computers for operating the OPAL-RT platform

TABLE I
MAIN PARAMETERS OF THE REDUCED-SCALE MMC PROTOTYPES

Converter parameters	Reference	18 HB model
Rated power	1059MVA	60 kVA
Rated DC voltage	640 kV	700V
Rated AC voltage	333 kV	400V
Rated current	1836A	83A
Cells per arm	401 HB	18 HB
Nominal cell voltage	2 kV	44 V
Arm inductance	50 mH	1,4 mH
Cell capacitance	10 mF	19,8 mF

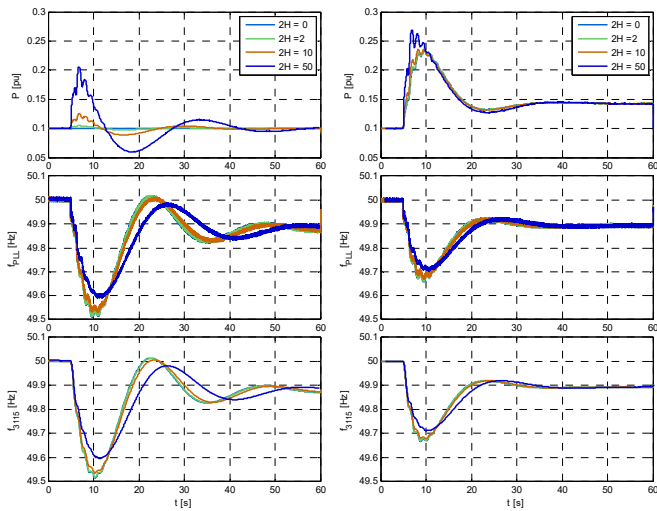
the sub-module voltage balancing are implemented on local FPGA based control boards, as further presented in [15].

V. EXPERIMENTAL RESULTS

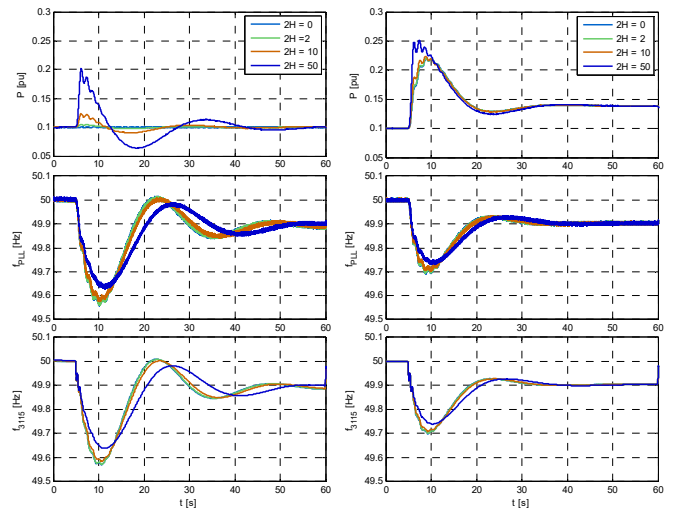
The effect of inertia support from an HVDC terminal has been tested by considering two separate scenarios where a load of 1000 MW has been applied to the nodes 5500 and 3115 of the Nordic 44 bus model from Fig. 1. The two different locations of the load are labelled as Case I and Case II, respectively. The two specified nodes have been selected to represent a condition where the load variation occurs close to the HVDC terminal (i.e. at node 5500) and at a significant distance from the HVDC terminal (i.e. at node 3115). The power injection from the converter is scaled in the P-HiL implementation so that 1.0 pu corresponds to 2800 MW.

The two investigated cases are tested in the experimental setup with different settings for the emulated inertia constant and the frequency droop gain. The values considered for the inertia are expressed with a value for $T_a (=2H)$ ranging from 0 to 50 s, where 0 corresponds to no inertial support. The frequency droop coefficient is also changed, with values in the range from 0 to 25.

For Case I, the power injected to the simulated power system model from the converter, the frequency measured by the PLL of the converter and the simulated frequency (i.e.



a) Experiments with $k_{ew} = 0$ b) Experiments with $k_{ew} = 20$
Fig. 5. Response of Case I with load step close to the HVDC terminal



a) Tests Experiments with $k_{ew} = 0$ b) Experiments with $k_{ew} = 20$
Fig. 8. Response of Case II with load step at bus 3115

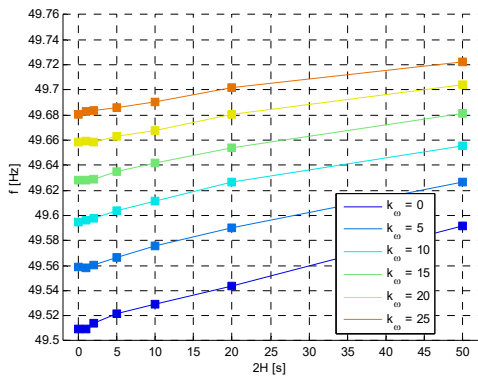


Fig. 6. Local frequency Nadir at the HVDC Converter terminal as function of virtual inertia for Case I

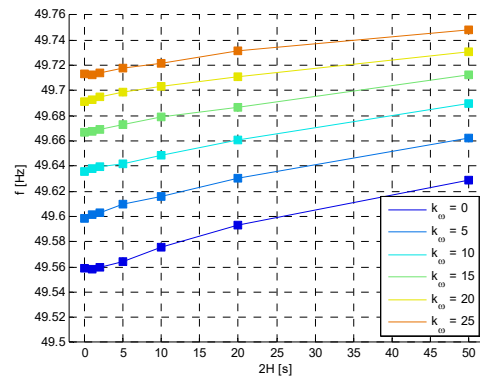


Fig. 9. Local frequency Nadir at the HVDC Converter terminal as function of virtual inertia for Case II

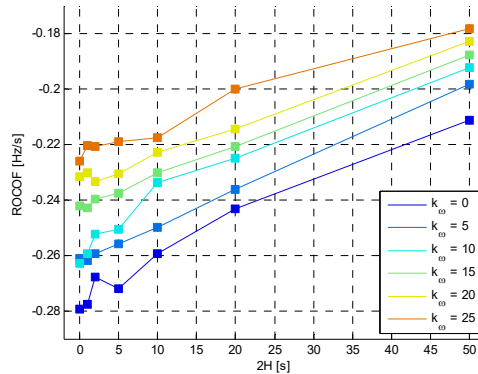


Fig. 7. Maximum ROCOF over 500 ms at the HVDC converter terminal as function of virtual inertia for Case I

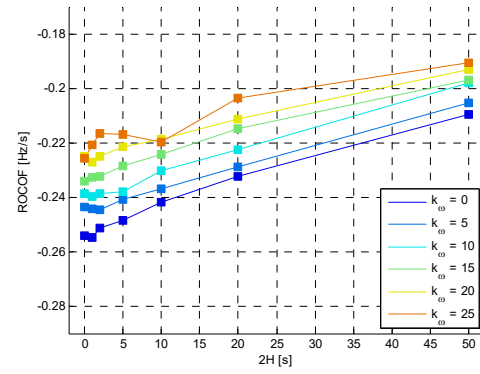


Fig. 10. Maximum ROCOF over 500 ms at the HVDC converter terminal as function of virtual inertia for Case II

the speed of a local generator) at node 3115 are presented in Fig. 5. Examples of results for various inertia values with a droop gain of 0 are shown in Fig. 5 a), while results with a droop gain of 20 are shown in Fig. 5 b).

As seen from the results in Fig. 5, changes in the inertia value do not affect the steady state power flow or frequency, but influence the transient response of the converter as well as the rest of the power system. Increasing the emulated inertia increases the peak power provided by the converter which again helps to support the grid frequency during the transient response to the load step. However, very high values also cause some faster oscillations in the power flow.

By contrast, the droop coefficient affects both the steady state operation and the peak of the power injection. Because the droop response of the converter is much faster than the

inertial dynamics of the power system, an increased droop coefficient increases the power support during the transient, leading to a further improvement of the frequency Nadir. Furthermore, the droop coefficient also affects the damping of the system, and the transient response settles in a shorter time for the cases with a higher droop coefficient.

From the results in Fig. 5 a), it can be clearly seen that the converter reaction to the load transient is negligible if the inertia and the droop gain are set to zero. On the other hand, the highest value for the inertia ($2H = 50$ s) leads to a peak power of approximately 0.2 pu, which is increased to 0.25 pu when combined with the droop. This is reflected in the frequency Nadir observed at the converter terminal, which is improved from 49.6 Hz to 49.7 Hz. The impact on the frequency Nadir from every combination of inertia constant

and droop gain is summarized in Fig. 6. This figure clearly shows how the Nadir is improved by increasing the inertia constant and the droop gain. Similarly, the maximum ROCOF detected as the discrete derivative over a time window of 500 ms is displayed in Fig. 7. The ROCOF values are negative, indicating the frequency drop due to the added load. Although local transients at higher frequencies are influencing the detected ROCOF at the converter terminal for low values of the inertia constant, the figure clearly confirms how increased values of the emulated inertia and increased droop gains contributes to a reduced maximum ROFOC in the grid.

For Case 2, the same load variation is applied to the node 3115, which is geographically distant from the bus where the studied HVDC converter is connected. Examples of time-domain results are shown in Fig. 8 while the frequency Nadir and the maximum value of the ROCOF for all investigated combinations of inertia constants and droop gains are shown in Fig. 9 and Fig. 10, respectively. From a qualitative perspective, the results appear very similar to the previous case, confirming the role of the emulated inertia constant and the droop gain in influencing the frequency dynamics of the power system. However, compared with the results from Case 1, it can be noted that the impact from the converter operation is slightly reduced since the distance partly delays and mitigates the effect of the load transient as observed from the bus where the converter terminal is connected.

VI. CONCLUSION

Future transmission systems are expected to experience challenges with reduced physical inertia, which can threaten operational reliability unless preventive measures are introduced. For this purpose, HVDC interconnections can be equipped with the capability for providing virtual inertia as an ancillary service. This paper presented an assessment of how an HVDC converter terminal integrated in the Nordic power system can provide synthetic inertia with a control strategy based on detection of the grid frequency derivative. The analysis is based on a reduced-scale laboratory setup for P-HiL testing, where a real-time simulation of the Nordic 44-bus model is combined with a MMC prototype representing a scaled model of an HVDC terminal. The results highlight the effect of the emulated inertia constant and the droop gain on the frequency transients in the power system, including evaluation of the grid frequency Nadir and the maximum Rate-of-Change-of-Frequency (ROCOF). The presented results demonstrate how both increased droop coefficient and higher inertia constant can help to improve the power system frequency transient in response to a large load step. However, very high values of inertia constant can lead to power oscillations while higher values of the droop coefficient lead to a more damped response.

REFERENCES

- [1] P. Tielens, D. Van Hertem, "The relevance of inertia in power systems," in *Renewable and Sustainable Energy Reviews*, Vol. 55, March 2016, pp. 999-1009
- [2] A. Ulbig, T. S. Borsche, G. Andersson, "Impact of Low Rotational Inertia on Power System Stability and Operation," in *Proc. of the 19th World Congress of the International Federation of Automatic Control*, Cape Town, South Africa, 24-29 August 2014, 8 pp.
- [3] B. Hartmann, I. Vokony, I. Táci, "Effects of decreasing synchronous inertia on power system dynamics – Overview of recent experiences and marketisation of services," in *International Transactions on Electrical Energy Systems*, Vol. 29, No. 12, December 2019, 14 pp.
- [4] J. O'Sullivan, A. Rogers, D. Flynn, P. Smith, A. Mullane, M. O'Malley, "Studying the Maximum Instantaneous Non-Synchronous Generation in an Island System – Frequency Stability Challenges in Ireland," in *IEEE Transactions on Power Systems*, Vol. 29, No. 6, Nov. 2014, pp. 2943-2951
- [5] M. Yu, A. Dyško, C. Booth, A. Roscoe, J. Zhu, H. Urdal, "Investigations on the Constraints relating to Penetration of Non-Synchronous Generation (NSG) in Future Power Systems," in *Proceedings of the 2015 Protection, Automation and Control (PAC) World Conference*, Glasgow, UK, 29 June – 2 July 2015, 9 pp.
- [6] Y. Wang, V. Silva, M. Lopez-Botet-Zulueta, "Impact of high penetration of variable generation on frequency dynamics in the continental Europe interconnected system," in *IET Renewable Power Generation*, Vol. 10, No. 1, January 2016, pp. 10-16
- [7] Statnett, Fingrid, Energinett and Svenka Kraftnät, "Challenges and opportunities for the Nordic power system," August, 2016.
- [8] H.-P. Beck, R. Hesse, "Virtual Synchronous Machine," in *Proceedings of the 9th International Conference on Electrical Power Quality and Utilisation*, Barcelona, Spain, 9-11 October 2007, 6 pp.
- [9] Q.-C. Zhong, G. Weiss, "Synchronverters: Inverters That Mimic Synchronous Generators," *IEEE Transactions on Industrial Electronics*, vol. 58, no. 4, April 2011, pp. 1259-1267
- [10] S. D'Arco, J. A. Suul, "Virtual Synchronous Machines – Classification of Implementations and Analysis of Equivalence to Droop Controllers for Microgrids," in *Proc. of IEEE PowerTech Grenoble 2013*, Grenoble, France, 16-20 June 2013, 7 pp.
- [11] Booth, G. P. Adam, A. J. Roscoe, C. G. Bright, "Inertia Emulation Control Strategy for VSC-HVDC Transmission Systems," in *IEEE Trans. on Power Systems*, Vol. 28, No. 2, May 2013, pp. 1277-1287
- [12] M. Guan, W. Pan, J. Zhang, Q. Hao, J. Cheng, X. Zheng, "Synchronous Generator Emulation Control Strategy for Voltage Source Converter (VSC) Stations," in *IEEE Transactions on Power Systems*, Vol. 30, No. 6, November 2015, pp. 3093-3101
- [13] E. Rakhshani, P. Rodriguez, "Inertia Emulation in AC/DC Interconnected Power Systems Using Derivative Technique Considering Frequency Measurement Effects," in *IEEE Transactions on Power Systems*, Vol. 32, No. 5, September 2017, pp. 3338-3351
- [14] R. Aouini, B. Marinescu, K. B. Kilani, M. Elleuch, "Synchronverter-Based Emulation and Control of HVDC Transmission," in *IEEE Trans. on Power Systems*, Vol. 31, No. 1, January 2016, pp. 278-286
- [15] S. D'Arco, G. Guidi, J. A. Suul, "Operation of a Modular Multilevel Converter Controlled as a Virtual Synchronous Machine," in *Proceedings of the International Power Electronics Conference, IPEC 2018 ECCE Asia*, Niigata, Japan, 20-24 May 2018, 8 pp.
- [16] P. C. Kotsampopoulos, F. Lehfuss, G. F. Lauss, B. Bletterie, N. D. Hatziairyiou, "The Limitations of Digital Simulation and the Advantages of PHIL Testing in Studying Distributed Generation Provision of Ancillary Services," in *IEEE Transactions on Industrial Electronics*, Vol. 62, No. 9, September 2015, pp. 5502-5515
- [17] S. H. Jakobsen, L. Kalembe and E. H. Solvang, "The Nordic 44 test network". https://figshare.com/projects/Nordic_44/57905
- [18] L. Vanfretti, T. Rabuzin, M. Baudette, and M. Murad, "iTesla power systems library (iPSL): A modelica library for phasor time-domain simulations," *SoftwareX*, vol. 5, pp. 84-88, 2016.
- [19] S. M. Hamre, "Inertia and FCR in the Present and Future Nordic Power System- Inertia Compensation," NTNU Master thesis, 2015.
- [20] Entso-e report, "Future system inertia," 2015.
- [21] T. D. Duong, S. D'Arco and J. O. Tande, "Architecture and laboratory implementation of a testing platform for Wide Area Monitoring Systems," in *Proc. IEEE 45th Ann. Conf. of the Ind. Electron. Soc.*, IECON'2019, Lisbon, Portugal, 14-17 October 2019, pp. 6419-6424
- [22] J. A. Suul, S. D'Arco, "Comparative Analysis of Small-Signal Dynamics in Virtual Synchronous Machines and Frequency-Derivative-Based Inertia Emulation," in *Proceedings of the 18th International Conference on Power Electronics and Motion Control, PEMC 2018*, Budapest, Hungary, 26-30 August 2018, pp. 344-351
- [23] J. Freytes, G. Bergna, J. A. Suul, S. D'Arco, H. Saad, X. Guillaud, "State-space modelling with Steady-State Time Invariant Representation of Energy Based Controllers for Modular Multilevel Converters," in *Proceedings of the 12th IEEE PES PowerTech Conference*, Manchester, UK, 18-22 June 2017, 7 pp.
- [24] S. D'Arco, T. T. Nguyen, J. A. Suul, "Evaluation of Virtual Inertia Control Strategies for MMC-based HVDC Terminals by P-HiL Experiments," in *Proc. IEEE 45th Ann. Conf. of the Ind. Electron. Soc.*, IECON'2019, Lisbon, Portugal, 14-17 Oct. 2019, pp. 4811-4818